PERGAMON

Acta mater. Vol. 47, No. 17, pp. 4449–4459, 1999
© 1999 Acta Metallurgica Inc.
Published by Elsevier Science Ltd. All rights reserved.
Printed in Great Britain
PII: S1359-6454(99)00229-3
1359-6454/99 $20.00 + 0.00

INTERFACIAL ADSORPTION IN TERNARY ALLOYS

C. HUANG[1, 2], M. OLVERA DE LA CRUZ[2]† and P. W. VOORHEES[2]

[1]National Taiwan University of Science and Technology, 43 Keelung Road, Section 4, Taipei, Taiwan 106 and [2]Department of Materials Science and Engineering, 2225 N. Campus Road, Northwestern University, Evanston, IL 60208, U.S.A.

(Accepted 13 April 1999)

Abstract—Interfaces of A–B–C ternary alloys decomposed into two and three phases are studied. The effect of the gradient energy coefficients $\bar{\kappa}_{II}$, I = A, B, C, on the interface composition profiles of ternary alloys is examined. The adsorption of component C in ternary alloys is obtained numerically by finding steady-state solutions of the nonlinear Cahn–Hilliard equations and by solving the two Euler–Lagrange equations resulting from minimizing the interfacial energy, and analytically near the critical point. It is found that the solutions from both numerical methods are identical for a two-phase system. In symmetric ternary systems (equal interaction energy between each pair of components) with a minority component C, the gradient energy coefficient of C, $\bar{\kappa}_{CC}$, can have a very strong influence on the degree of adsorption. In the α and β two-phase regions, where α and β are the phases rich in the majority components A and B, respectively, as $\bar{\kappa}_{CC}$ increases, the adsorption of the minority component C in the α and β interfaces decreases. Near a critical point, however, the degree of adsorption of minority component C is independent of the gradient energy coefficient. © *1999 Acta Metallurgica Inc. Published by Elsevier Science Ltd. All rights reserved.*

Keywords: Interface; Thermodynamics; Spinodal decomposition; Phase equilibria

1. INTRODUCTION

Many commercial alloys are multicomponent and undergo phase separation. The morphology of the phases, and in particular the interfaces, determines the mechanical properties of these multiple-phase materials. Therefore, the interfaces that develop during the dynamics of phase separation play a very important role in commercial applications.

The microstructures and interfaces are a consequence of both the thermodynamics and dynamics of phase separation. While phase separation dynamics for systems undergoing spinodal decomposition have been extensively studied in binary alloys [1], only a few studies exist in ternary alloys. For example, the thermodynamic stability and the early stages of phase separation dynamics in ternary alloys were analyzed extending the linearized Cahn–Hilliard equations for binary systems [2–4]. Furthermore, the nonlinear dynamics of the inhomogeneous morphological evolution during the spinodal decomposition process have been studied recently [5, 6]. To our knowledge, however, there has been no complete study of the properties of interfaces in ternary alloys.

Ternary A–B–C mixtures can decompose into two or three phases. Between any two phases rich in components I and J, the third component K segregates in the interface, even when the equilibrium composition of component K is equal in both phases [5–10]. The adsorption effect has a strong influence on the decomposition patterns into two and three phases. It can in principle enhance the stability of these phases by lowering the interfacial energy and increasing the interfacial thickness [7–10].

In this paper we study the interfacial properties, such as the interfacial energy and the interfacial thickness, when a third minority component C is added to A and B binary mixtures. Equilibrium interface profiles are obtained for a ternary mixture segregating into a two-phase A-rich and B-rich region, by minimizing the interfacial energy. We find the degree of adsorption of C. We also analyze the interfaces in the three-phase region. Our results are compared with the steady-state solutions of the nonlinear Cahn–Hilliard equations (NLCH).

Consider a ternary A–B–C system described by the free energy per lattice site on mixing

$$\Delta f = \Delta f_0 + \sum_{\mathrm{I=A,\,B,\,C}} \bar{\kappa}_{\mathrm{II}} (\nabla \varphi_{\mathrm{I}})^2 \qquad (1)$$

where Δf_0 is the regular solution model free energy per lattice site, and $\bar{\kappa}_{\mathrm{II}}$ is the bare gradient energy coefficient of component I reflecting the unfavorable nature of compositional inhomogeneities. Δf_0 is a function of the local compositions of component I, $\varphi_{\mathrm{I}}(\mathbf{r})$, I = A, B, and C

†To whom all correspondence should be addressed.

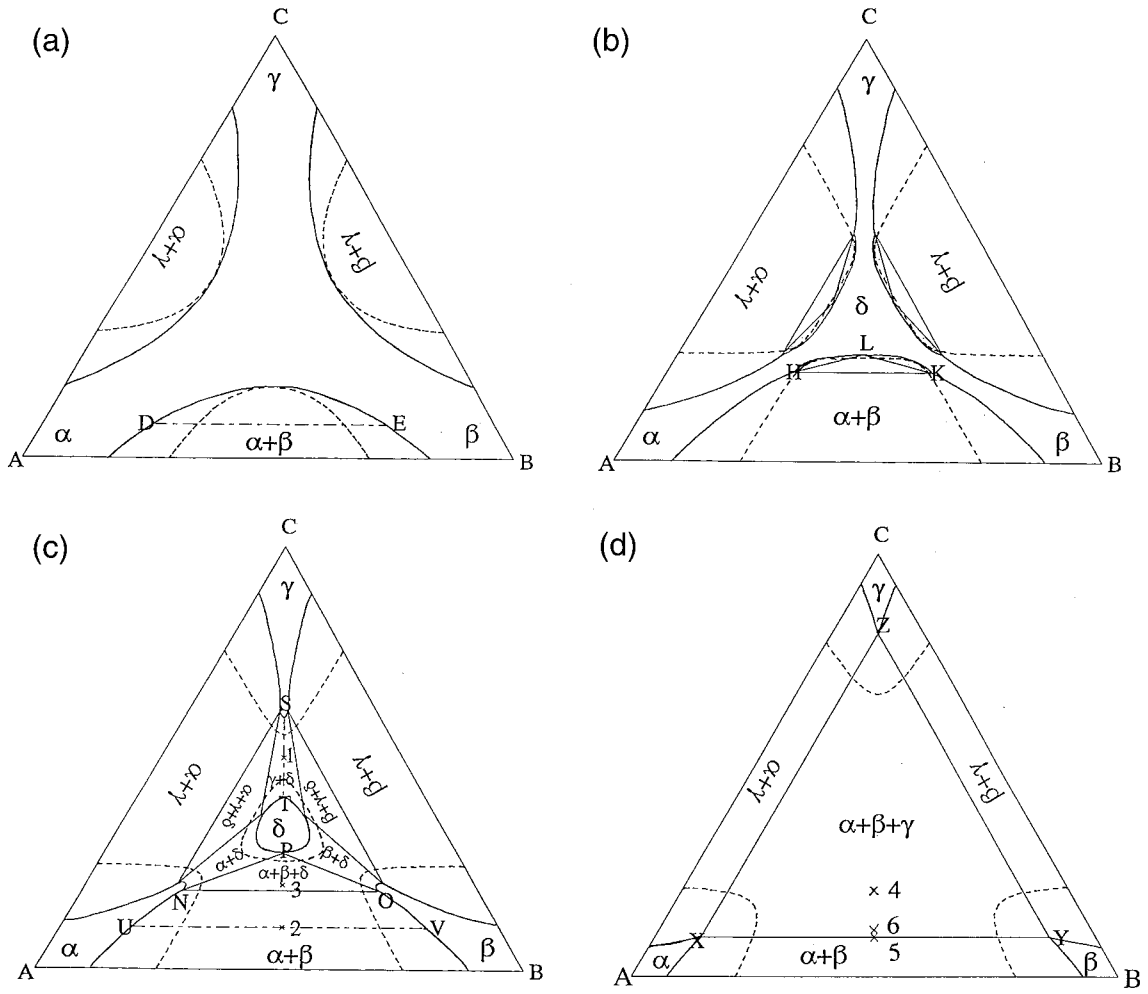

Fig. 1. The phase diagrams of symmetric ternary systems for (a) $\chi = 2.4$, (b) $\chi = 2.65$, (c) $\chi = 2.7$, and (d) $\chi = 3.0$. The symbols (- - - -) and (– · –) correspond to the spinodal curves and the tie-lines, respectively.

$$\frac{\Delta f_0}{k_B T} = \varphi_A \ln \varphi_A + \varphi_B \ln \varphi_B + \varphi_C \ln \varphi_C + \chi_{AB}\varphi_A\varphi_B + \chi_{BC}\varphi_B\varphi_C + \chi_{AC}\varphi_A\varphi_C \quad (2)$$

where $\mathbf{r}$ is a position vector, χ_{IJ} is the effective interaction energy between components I and J, given by $\chi_{IJ} = \omega_{IJ}/k_B T$, where ω_{IJ} is the regular solution coefficient between species I and J, k_B is Boltzmann's constant, and T is temperature. The phase diagrams of ternary polymer blends constructed in Refs [7, 8] are appropriate in describing ternary alloys by setting N_I, the degree of polymerization of component I, I = A, B, C, equal to one. The gradient energy coefficients $\bar{\kappa}_{II}$ in equation (1) of alloys, however, can be much smaller than those of polymers, leading to larger degrees of adsorption. Therefore, the linearized solution of the Euler–Lagrange (E–L) equations that result from the minimization of the interfacial energy found in Refs [9, 10] cannot always describe ternary alloys. In this paper, the non-linear E–L equations are solved. Though the interfacial properties found in ternary polymer blends do not always describe the interfacial properties of alloys, the kinetics of phase separation and the dynamic scaling laws found in Refs [7–10] are the same in alloys. Indeed, the phenomenological results on the kinetics of phase separation in ternary alloys found recently [11], are in agreement with the results in polymer blends. While in polymer blends, $\bar{\kappa}_{II}$ are composition dependent terms arising from the nonlocality of polymer configurational entropy, in alloys the $\bar{\kappa}_{II}$ are due mostly from the short-range atomic interactions, and thus must be determined via a quantum mechanical calculation. We take the gradient energy coefficients to be constants.

In Section 2, we briefly describe the thermodynamics and the dynamics of phase separation for ternary systems. In Section 3, we describe the two numerical techniques we use to obtain the interface profiles; we solve (i) the non-linear Cahn–Hilliard equations in the long time limit, and (ii) the Euler–

Lagrange equations resulting from minimizing the interfacial energy. In this section we also describe a Landau-type approach to determine the degree of adsorption of the minority C component at the A-rich and B-rich interfaces valid around the critical points of transitions to two phases. In these regions of the ternary phase diagram, we find that the adsorption of the minority C component is low and independent of the gradient energy coefficients. The gradient energy coefficients of ternary alloys have large effects when the system is strongly segregated. The results and discussion regarding these effects are given in Section 4. In Section 5 we summarize our studies.

2. THERMODYNAMICS AND DYNAMICS OF PHASE SEPARATION IN TERNARY SYSTEMS

For simplicity, we determine here the phase diagrams of symmetric ternary alloys, i.e. alloys with $\omega_{AB} = \omega_{BC} = \omega_{AC} = \omega$ ($\chi_{AB} = \chi_{BC} = \chi_{AC} = \chi$). The phase diagrams and the spinodal curves for symmetric ternary systems are shown in Fig. 1 for different values of χ. Note that as T decreases χ increases. The details on how to calculate the phase diagrams and the spinodal curves from the free energy function per lattice site in a homogeneous system, Δf_0 as given in equation (2), can be found in Refs [7, 8].

For $\chi < 2$, the ternary system is homogeneous for any alloy, or mean, composition ($\bar{\varphi}_A, \bar{\varphi}_B, \bar{\varphi}_C$). A typical ternary phase diagram is shown in Fig. 1(a), where $\chi = 2.4$. This diagram is qualitatively the same in terms of the morphology of the two-phase region for $2 \le \chi < 2.57$. In the diagram the A-rich, B-rich, and C-rich phases are labeled as α, β, and γ, respectively. As χ increases from 2.0, there are three lines of critical points in a temperature vs composition diagram given by $(1/\chi, 1/\chi, 1 - 2/\chi)$, $(1 - 2/\chi, 1/\chi, 1/\chi)$, and $(1/\chi, 1 - 2/\chi, 1/\chi)$, determined by the intersection of the spinodal lines with the coexistence curves in each $\alpha+\beta$, $\beta+\gamma$, and $\alpha+\gamma$ region. The tie lines, which give the equilibrium compositions in the two-phase regions, are parallel to the I–J axis. For example, for any alloy composition along the line DE in Fig. 1(a) the equilibrium compositions of α and β are given by $D = (\bar{\varphi}_A^{\alpha}, \bar{\varphi}_B^{\alpha}, \bar{\varphi}_C^{\alpha})$ and $E = (\bar{\varphi}_A^{\beta}, \bar{\varphi}_B^{\beta}, \bar{\varphi}_C^{\beta})$, where $\bar{\varphi}_C^{\alpha} = \bar{\varphi}_C^{\beta} = \bar{\varphi}_C$.

When $\chi > 2.57$ three-phase regions appear in the phase diagrams. The single-phase region near the center of the composition triangle is labeled as δ. There are three three-phase regions, inside the small triangles shown in Fig. 1(b) where $\chi = 2.65$. As expected by the phase rule, each three-phase region is separated from single-phase regions by two-phase regions on the right and left of each small triangle. These six new two-phase regions each have a critical point (as χ increases, they generate six lines of critical points emerging from the critical points at $\chi = 2.57$). For example, for any initial composition inside the triangle HKL, with equilibrium compositions given by $H = (\bar{\varphi}_A^{\alpha}, \bar{\varphi}_B^{\alpha}, \bar{\varphi}_C^{\alpha})$, $K = (\bar{\varphi}_A^{\beta}, \bar{\varphi}_B^{\beta}, \bar{\varphi}_C^{\beta})$, and $L = (\bar{\varphi}_A^{\delta}, \bar{\varphi}_B^{\delta}, \bar{\varphi}_C^{\delta})$, the left- and right-hand sides of the tie-triangle HKL are $\alpha+\delta$ and $\beta+\delta$, respectively. When $\chi = 8/3$, the critical lines of $\alpha+\delta$, $\beta+\delta$, and $\gamma+\delta$ join at (0.5, 0.25, 0.25), (0.25, 0.5, 0.25), and (0.25, 0.25, 0.5), respectively. For $\chi > 8/3$ these two-phase regions overlap and all the critical points disappear as shown in Fig. 1(c) for $\chi = 2.7$. When χ is 2.7456, the three-phase regions shown in Fig. 1(c) touch at the center of the ABC triangle. For $\chi > 2.7456$ they overlap leading to a single interior α, β, and γ three-phase triangle with equilibrium compositions given by the points X, Y, and Z, shown in Fig. 1(d) for $\chi = 3.0$.

The dynamics of phase separation for ternary systems are studied solving the two non-linear diffusion equations, given by [7, 8]

$$\begin{aligned}\frac{\partial}{\partial t}\left[\varphi_I(r,t)\right] &= M_{II}\nabla^2\left(\mu^s_{0,I} - \mu^s_{0,C} - 2\kappa_{II}\nabla^2\varphi_I - 2\kappa_{IJ}\nabla^2\varphi_J\right) \\ &\quad + M_{IJ}\nabla^2\left(\mu^s_{0,J} - \mu^s_{0,C} - 2\kappa_{JI}\nabla^2\varphi_I - 2\kappa_{JJ}\nabla^2\varphi_J\right) \\ &\quad I \neq J;\ I, J = A, B. \end{aligned} \tag{3}$$

Here we have eliminated the variable $\varphi_C(r, t)$ since $\varphi_A + \varphi_B + \varphi_C = 1$ and have used the Gibbs–Duhem relationship locally. These equations are derived in Appendix A in Refs [7, 8]. In equation (3), $\mu^s_{0,I} = \partial \Delta f_0 / \partial \varphi_I$ is an effective diffusion potential of component I, $\kappa_{II} = \bar{\kappa}_{II} + \bar{\kappa}_{CC}$ and $\kappa_{AB} = \bar{\kappa}_{CC}$ are the effective coefficients of the gradient energy terms in the free energy when the component C is eliminated, and $M_{II} = (1 - \bar{\varphi}_I)^2 M_I + \bar{\varphi}_I^2 \sum_{J \neq I} M_J$, I = A, B, and $M_{AB} = -(1 - \bar{\varphi}_A)\bar{\varphi}_B M_A - (1 - \bar{\varphi}_B)\bar{\varphi}_A M_B + \bar{\varphi}_A \bar{\varphi}_B M_C$, where M_I, the Onsager coefficient of I, are effective mobilities.

In Refs [7, 8] we analyzed the dynamics of ternary systems with $\bar{\varphi}_A = \bar{\varphi}_B$ decomposing into two and three phases. We solved equation (3) in two dimensions using periodic boundary conditions until the very late stages of the decomposition process or steady state, where the interfacial properties are time independent. Here we analyze only the interfaces in the steady state as a function of $\bar{\kappa}_{II}$ and by using the numerical methods described in Section 3. In order to study the effect of the gradient energy coefficients $\bar{\kappa}_{II}$ on the interface profiles, we vary the two parameters, e_1 and e_2, which are defined as

$$e_1 = \frac{\bar{\kappa}_{BB}}{\bar{\kappa}_{AA}} \tag{4a}$$

$$e_2 = \frac{\bar{\kappa}_{CC}}{\bar{\kappa}_{AA}}. \tag{4b}$$

3. THE LIMIT OF SMALL ADSORPTION

The adsorption of the third minority component C along the interfaces between the two majority components A- and B-rich phases increases the interfacial thickness and decreases the interfacial energy [9, 10]. The degree of adsorption near the critical points when the interactions between A and C and B and C are equal (non-selective C component) is a simple function of the thermal energy and the alloy composition only; that is, it is independent of the gradient energy coefficients, and it can be obtained with a linearized analysis of the interfacial energy [9, 10], which is possible when the degree of adsorption is low. We now present a nonlinear Landau-type analysis of adsorption near critical points where there is only a linearized coupling between the fluctuations of C and both A and B. In the presence of a non-selective C component with $\chi_{AC} = \chi_{BC} = \eta\chi_{AB}$, where η is a constant >0, the adsorption of C per interfacial thickness in the α and β interfaces is defined in two dimensions as

$$\Gamma_C = \frac{1}{L}\int_{-\infty}^{\infty} (\varphi_C(r) - \bar{\varphi}_C^e)\, dx \tag{5a}$$

where $\bar{\varphi}_C^e = \bar{\varphi}_C^\alpha = \bar{\varphi}_C^\beta$, Γ_C is a dimensionless adsorption, L is the interfacial thickness defined as [9, 10]

$$L = \frac{2(\varphi_C(0) - \bar{\varphi}_C)}{\left|\frac{d\varphi_C}{dx}\right|_{max}} \tag{5b}$$

and $|d\varphi_c/dx|_{max}$ is the maximum of the absolute value of $d\varphi_c/dx$. Note that since φ_c^e is equal in the two phases, Γ_c is independent of the location of the dividing surface in a Gibbsian model of the interface. The general case is treated in Refs [7, 8]. In non-selective C systems with no interactions between A and C and B and C ($\chi_{AC} = \chi_{BC} = 0$), one would expect C to segregate in the interfaces between α and β phases to decrease the bonds between A and B. In the general case the adsorption of non-selective ($\chi_{AC} = \chi_{BC} = \eta\chi_{AB}$, $\eta \neq 0$) minority components C in the α and β interfaces as a function of $\bar{\varphi}_C$, $\bar{\varphi}_C < \bar{\varphi}_A = \bar{\varphi}_B$, can be understood by analyzing the contribution to the free energy from infinitesimal compositional fluctuations. A Taylor's series expansion of Δf in the Fourier components of $\psi_1(r) = (\delta\varphi_A(r) - \delta\varphi_B(r))/(2\bar{\varphi})$ and $\psi_2(r) = -\delta\varphi_C(r)$, where $\bar{\varphi} = \bar{\varphi}_A + \bar{\varphi}_B$, and $\delta\varphi_I(r) = \varphi_I(r) - \bar{\varphi}_I$, I = A, B, C, in systems with $\bar{\varphi}_A = \bar{\varphi}_B$ is given by

$$\begin{aligned}\Delta f(\{\psi_1(k), \psi_2(k)\}) \sim & \sum_{I=1,2}\sum_k \frac{\Omega_{II}(k)}{2}\psi_I^2(k) \\ & + \sum_{k,k',k''} \frac{\Omega_{112}}{3!}\delta(k + k' \\ & + k'')\psi_1(k)\psi_1(k')\psi_2(k'') \\ & + \sum_{k,k',k'',k'''} \frac{\Omega_{1111}}{4!}\delta(k + k' + k'' \\ & + k''')\psi_1(k)\psi_1(k')\psi_1(k'')\psi_1(k''')\end{aligned} \tag{6}$$

where

$$\Omega_{11}(k) = \bar{\varphi}^2(4/(\bar{\varphi}) - 2\chi_{AB} + 4\bar{\kappa}_{AA}k^2) \tag{6a}$$

$$\Omega_{22}(k) = 1/(\bar{\varphi}(1-\bar{\varphi})) + (0.5 - 2\eta)\chi_{AB} + (\bar{\kappa}_{AA} + 2\bar{\kappa}_{CC})k^2 \tag{6b}$$

$$\Omega_{112} = -12 \tag{6c}$$

$$\Omega_{1111} = 32\bar{\varphi}. \tag{6d}$$

The sign of the coefficients $\Omega_{11}(k=0)$ and $\Omega_{22}(k=0)$ determine the instability with respect to the formation of $\alpha+\beta$ mixtures and γ phase, respectively. Let us assume that the system is unstable to the formation of two phases, one rich in A (α) and the other rich in B (β), and stable to the formation of a phase rich in the minority C (γ) ($\Omega_{11}(k=0) < 0$ and $\Omega_{22}(k=0) > 0$). This is the case, for example, along the line halfway and perpendicular to the A–B side of the triangle shown in Fig. 1(a) inside the two-phase region. Since C is non-selective, $\bar{\varphi}_C$ is constant in the two bulk phases far from the interface, since the phases are compositionally uniform. However, the third-order term Ω_{112} in equation (6) will induce a composition fluctuation in C whenever there is a composition fluctuation of A and B. Indeed, for a single wave compositional fluctuation of wavelength $\lambda_1 = 2\pi/k_1$, $\psi_1(r) = A_1 e^{i\vec{k}_1\cdot\vec{r}} + c.c.$, if $\chi_{AB} > 2/\bar{\varphi} + 2\bar{\kappa}_{AA}k_1^2$ a compositional fluctuation in $\psi_2(r) = A_2 e^{i\vec{k}_2\cdot\vec{r}} + c.c.$ of half wavelength, $k_2 = 2k_1$, is induced by the negative Ω_{112} term in equation (6), which is non-zero only if $k' + k'' + k''' = 0$ with $k' = k_1$, $k'' = k_1$, $k''' = k_2$. For this periodic interface profile with a single wavenumber fluctuation in both components A and B, the composition of the minority C is largest at the points where the composition fluctuations of A and B are at a minimum (i.e. where $\delta\varphi_I(r) = 0$, I = A, B). This implies that there is an excess of C at the interfaces. While this is the situation near the critical point where the interfaces are very diffuse, this can also occur at the very early stages of spinodal decomposition where the decomposition process is dominated by composition fluctuations of A and B of a single wavelength with the maximum growth rate as given by the linear Cahn theory. In this case, this fluctuation

of A and B will induce an out-of-phase composition fluctuation of C with half wavelength. This induced composition fluctuation of C is indeed observed during the dynamics of phase separation into shallow quenches and/or when the degree of adsorption of C is small, e.g. when the gradient energy coefficients are large (e.g. in ternary polymer blends [9, 10]). The magnitude of the adsorption in steady state, when the composition has evolved to form two macroscopic phases (i.e. for infinite wavelengths, $k_1 = 0$), can be obtained by minimizing equation (6). This gives the most probable amplitude of the induced compositional fluctuation in C, $\bar{A}_2$, that is also proportional to the square of the amplitude of the composition fluctuation of A and B, leading to

$$\bar{A}_2 = \frac{\Omega_{11}(k_1)\Omega_{112}}{\Omega_{1111}\Omega_{22}(k_2) - \Omega_{112}^2/3} \tag{7}$$

with $k_1 = 0$ and $k_2 = 0$. The degree of adsorption of C for a composition fluctuation of A and B of a single wavelength near the critical points is obtained substituting $\psi_2(r) = A_2\, e^{i\vec{k}_2\cdot\vec{r}} + \text{c.c.}$ with the amplitude given by equation (7) in equations (5a) and (5b), leading to an adsorption proportional to $\bar{A}_2$. Therefore, the adsorption of a non-selective minority C, $\chi_{AC} = \chi_{BC} = \eta\chi_{AB}$, is minimum when $\eta = 0$, and it increases as η increases, since the other terms in Ω_{22} are greater than zero. When η increases such that $\Omega_{1111}\Omega_{22}(k_2 = 0) - \Omega_{112}^2/3 < 0$, however, three phases will appear at steady state, as shown in Fig. 1(b) for $\eta = 1$. Equations (6) and (7) cannot be used to describe deep quenches in the steady state when the compositional fluctuations are not small because the Landau-type expansion cannot be truncated at fourth order in the composition fluctuations in this limit and because the mass conservation laws are not included in our analysis. These equations suggest that Γ_c in equation (7), proportional to $\bar{A}_2$, is linear in $\bar{\varphi}_C$ for $\bar{\varphi}_C \ll \varphi_C^{crit}$. This can be found by expanding $\bar{A}_2$ for small $\bar{\varphi}_C$ in the limit $\bar{\varphi}_C \ll \bar{\varphi}_C^{crit}$ and using $\bar{\varphi} = 1 - \bar{\varphi}_C$. When η is small, however, a critical point appears when $\bar{\varphi}_C$ increases towards $\bar{\varphi}_C^{crit} = 1 - 2/\chi_{AB}$, and the adsorption of C near the critical point should decrease as $\bar{\varphi}_C$ increases, $\Gamma_C \sim \bar{A}_2(k_1 = 0) \sim \bar{\varphi}_C(1-\bar{\varphi}_C)(\bar{\varphi}_C^{crit} - \bar{\varphi}_C)$. Thus the adsorption of C is independent of the gradient energy coefficients. This suggests a maximum of the adsorption at a certain $\bar{\varphi}_C < \bar{\varphi}_C^{crit}$. The results are in good agreement with the solution of the NLCH equations in the steady state [9, 10].

The above linear-response analysis, however, breaks down for large degrees of adsorption, such as for ternary alloys having very small gradient energy coefficients. These compositional gradient terms have a very strong influence on the interfacial properties. For example, the terms are very important in determining the equilibrium interface composition profile. In this section we obtain the interface composition profile finding the minimum of the interfacial energy, and compare the results with those obtained solving the NLCH equations in one dimension in the steady state.

4. NUMERICAL METHODS

For a flat interface between the α- and β-phases of compositions $\bar{\varphi}_I^{\alpha}$ and $\bar{\varphi}_I^{\beta}$, respectively, the interfacial energy σ is given by the difference, per unit area of interface, between the actual free energy and that which it will have if the properties of the two phases were continuous [12]

$$\sigma = N_V \int_{-\infty}^{\infty} \left(\Delta f_0^{m} + \sum_{I=A,\,B,\,C} \bar{\kappa}_{II} \left(\frac{d\varphi_I}{dx} \right)^2 \right) dx \tag{8}$$

where N_V is the number of lattice sites per unit volume and

$$\Delta f_0^{m} = \Delta f_0(\varphi_I(x)) - \sum_I \varphi_I(x)\mu_{0,I}^{\alpha(\beta)}$$

where $\mu_{0,I}^{\alpha(\beta)}$ is the chemical potential evaluated at the bulk compositions of the equilibrium the α- and β-phases. The composition of C has been eliminated using the constraint, $\varphi_A(x) + \varphi_B(x) + \varphi_C(x) = 1$. Hence an extremum of σ in equations (4a) and (4b) is obtained solving simultaneously the resulting two Euler–Lagrange (E–L) equations [13]

$$\frac{\partial I}{\partial \varphi_A} - \frac{d}{dx}\left(\frac{\partial I}{\partial (d\varphi_A/dx)} \right) = 0 \tag{9a}$$

$$\frac{\partial I}{\partial \varphi_B} - \frac{d}{dx}\left(\frac{\partial I}{\partial (d\varphi_B/dx)} \right) = 0 \tag{9b}$$

where x is a position perpendicular to the interface

$$I = \Delta f_0^{m} + \sum_{I=A,\,B,\,C} \bar{\kappa}_{II} \left(\frac{d\varphi_I}{dx} \right)^2 - \lambda_1 (\varphi_A(x) - \bar{\varphi}_A) - \lambda_2 (\varphi_B(x) - \bar{\varphi}_B)$$

and λ_1, λ_2 are two Lagrange multiplier constants, included to assure that the global mass conservation constraints, i.e.

$$\int_{-\infty}^{\infty} (\varphi_I(x) - \bar{\varphi}_I)\, dx = 0, \quad I = A, B$$

are satisfied. The Lagrange multipliers $\lambda_1 = 0$ and $\lambda_2 = 0$ when the boundary conditions, $\Delta f_0^{m} = 0$ and $d\varphi_B/dx = d\varphi_B/dx = 0$ as $x \to \pm\infty$, are applied in equations (9a) and (9b). Hence, equations (9a) and (9b) reduce to

$$\frac{d^2\varphi_A}{dx^2} = \frac{1}{2(\kappa_{AA}\kappa_{BB} - \kappa_{AB}^2)}\left(\frac{\partial \Delta f_0^m}{\partial \varphi_A}\kappa_{BB} - \frac{\partial \Delta f_0^m}{\partial \varphi_B}\kappa_{AB}\right) \quad (10a)$$

$$\frac{d^2\varphi_B}{dx^2} = \frac{1}{2(\kappa_{AA}\kappa_{BB} - \kappa_{AB}^2)}\left(\frac{\partial \Delta f_0^m}{\partial \varphi_B}\kappa_{AA} - \frac{\partial \Delta f_0^m}{\partial \varphi_A}\kappa_{AB}\right). \quad (10b)$$

We solve equations (10a) and (10b) in one dimension by applying the equilibrium boundary conditions. These equations are solved numerically using COLSYS as a system of second-order non-linear ordinary differential equations [14].

We also determine numerically the steady-state interfacial composition profiles using the NLCH, equation (3), in one dimension with the equilibrium boundary conditions, $\varphi_I(x = \infty) = \bar{\varphi}_I^{\alpha}$ and $\varphi_I(x = -\infty) = \bar{\varphi}_I^{\beta}$, and $d\varphi_A/dx = d\varphi_B/dx = 0$ as $x \rightarrow \pm\infty$ (instead of periodic boundary conditions). We solve equation (3) in terms of reduced distance and time parameters, $x = (\omega/4\bar{\kappa}_{AA})^{1/2}r$ and $\tau = (M_{AA}\omega^2/4\bar{\kappa}_{AA})t$. The values of Δx and $\Delta\tau$ are chosen to satisfy the conditions for numerical stability and have sufficient numbers of meshpoints to resolve the composition profiles through the interface. To reach the steady-state solution efficiently, initial composition profiles are provided. For example, the initial composition profiles of a ternary system into two phases α and β assuming that each phase coarsens and reaches the equilibrium compositions are given by

$$\Delta\varphi_A(x) = \Delta\varphi_A^{\alpha} \tanh\left[-\left[\frac{2(\bar{\varphi}_A\chi - 1)}{\bar{\varphi}_A\chi(1 + e_1)}\right]^{1/2} x\right] \quad (11a)$$

$$\Delta\varphi_B(x) = \Delta\varphi_B^{\alpha} \tanh\left[-\left[\frac{2(\bar{\varphi}_B\chi - 1)}{\bar{\varphi}_B\chi(1 + e_1)}\right]^{1/2} x\right] \quad (11b)$$

$$\Delta\varphi_C(x) = 0 \quad (11c)$$

where $\Delta\varphi_I(x) = \varphi_I(x) - \bar{\varphi}_I$, and $\Delta\varphi_I^{\alpha} = \bar{\varphi}_I^{\alpha} - \bar{\varphi}_I$, I = A, B, C. Indeed, equations (11a)–(11c) are obtained analytically near critical points [12] when the adsorption of C is neglected. As discussed in Section 3, the adsorption in these regions is indeed negligible. Similarly for three-phase systems, between any two phases rich in components I and J, the compositions of I and J are taken to have initially tanh profiles. The initial forms of the composition profiles do not affect the steady-state interface profiles.

5. RESULTS AND DISCUSSION

We compare the interface profiles determined using the two E–L equations and the NLCH equations in the steady state. We find that the profiles determined from both methods are identical. However, we have not determined interfacial profiles in a system with three phases using the E–L equations. In this case, the solutions to the E–L equations are very sensitive to the initial guess, which frequently yields profiles that are not global minima. This sensitivity was not observed with the NLCH equations. We analyze systems with $\bar{\varphi}_C < \bar{\varphi}_A = \bar{\varphi}_B$ quenched into the two- and three-phase regions. In particular, the systems at points 5 and 6 with initial compositions (0.45275, 0.45275, 0.0945) and (0.45, 0.45, 0.1) at $\chi = 3.0$, see Fig. 1(d), are studied. System 5 is unstable to the formation of α and β with compositions given by $X = (0.811, 0.0945, 0.0945)$, and $Y = (0.0945, 0.811, 0.0945)$, respectively; while system 6 is unstable to the formation of the α- and β-phases and metastable to the formation of γ-phase with compositions given by X, Y, and $Z = (0.0945, 0.0945, 0.811)$, respectively.

In Figs 2(a)–(c), we show the composition profiles of system 5 for $e_2 = 0$, 1, and 10, respectively, when e_1 is fixed to be 1.0. As expected, when e_1 is equal to 1 (the gradient energy coefficients contributed from A and B are the same), the profiles $\varphi_A(x) = \varphi_B(-x)$ and $\varphi_C(x)$ is symmetric about $x = 0$. The composition of C is the largest at $x = 0$. As $\bar{\kappa}_{CC}(e_2)$ increases the value of $\Delta\varphi_C(x = 0)$ decreases and the interface becomes broader. When $\bar{\kappa}_{CC}(e_2) \rightarrow \infty$, since even an infinitesimal amount of C segregating in the interfaces increases the interfacial energy, we expect no adsorption of C along the interfaces. When e_1 is not equal to 1, $\varphi_A(x) \neq \varphi_B(-x)$ and therefore the symmetry of $\varphi_C(x)$ breaks down, as shown in Figs 2(d) and (e) at $e_1 = e_2 = 0$, and $e_1 = 50$, $e_2 = 1$, respectively. We find that the maximum adsorption of C [the largest $\Delta\varphi_C(x)$ value] occurs when $\bar{\kappa}_{CC} = \bar{\kappa}_{BB} = 0$ or $\bar{\kappa}_{CC} = \bar{\kappa}_{AA} = 0$.

The gradient energy coefficients not only affect the adsorption of the minority component C in the interfaces between the two majority A-rich and B-rich phases, but also have a strong influence on the formation of a third phase that is rich in the minority component C. In Figs 3–5, we plot the steady-state interface profiles of system 6 for $e_1 = e_2 = 0$, $e_1 = e_2 = 1$, and $e_1 = e_2 = 1$, $e_2 = 10$, respectively. The interfaces plotted on a larger scale are shown in parts (d) and (e) of each figure. The initial composition profiles used assume that the phases α, β, and γ form and that the γ-phase forms between the α- and β-phases, as shown in Fig. 6. In the case of $e_1 = e_2 = 0$ (see Fig. 3), the formation of each phase is observed in the steady state. We observe the adsorption of C in the interfaces between the

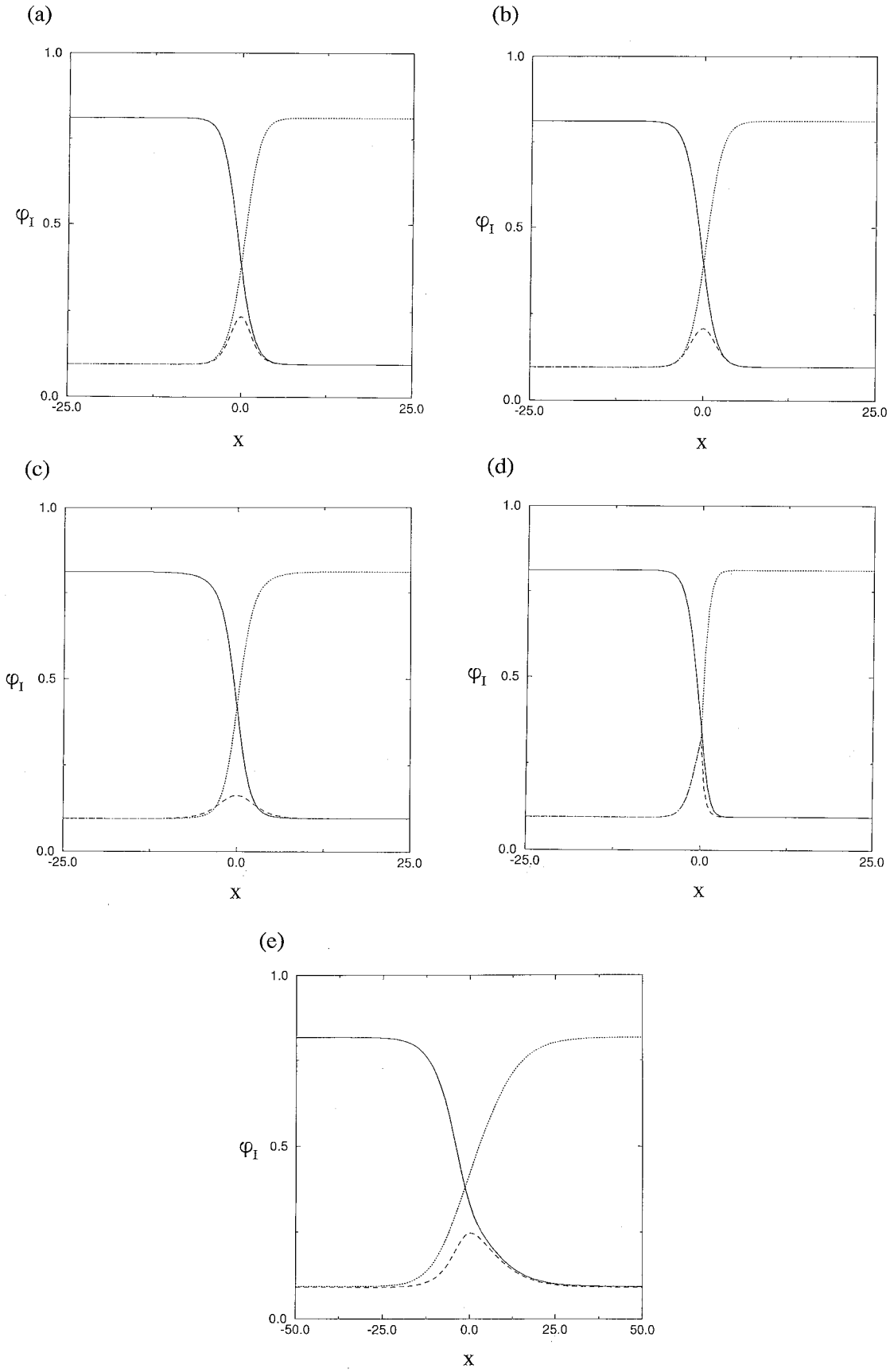

Fig. 2. Equilibrium composition profiles of system 5 in Fig. 1(d) for (a) $e_1 = 1$ and $e_2 = 0$, (b) $e_1 = 1$ and $e_2 = 1$, (c) $e_1 = 1$ and $e_2 = 10$, (d) $e_1 = 0$ and $e_2 = 0$, and (e) $e_1 = 50$ and $e_2 = 1$. The symbols (——), (· · · · · ·), and (- - - -) correspond to components A, B, and C, respectively. The values of x are in the unit of $(4\bar{\kappa}_{AA}/\omega)^{1/2}$.

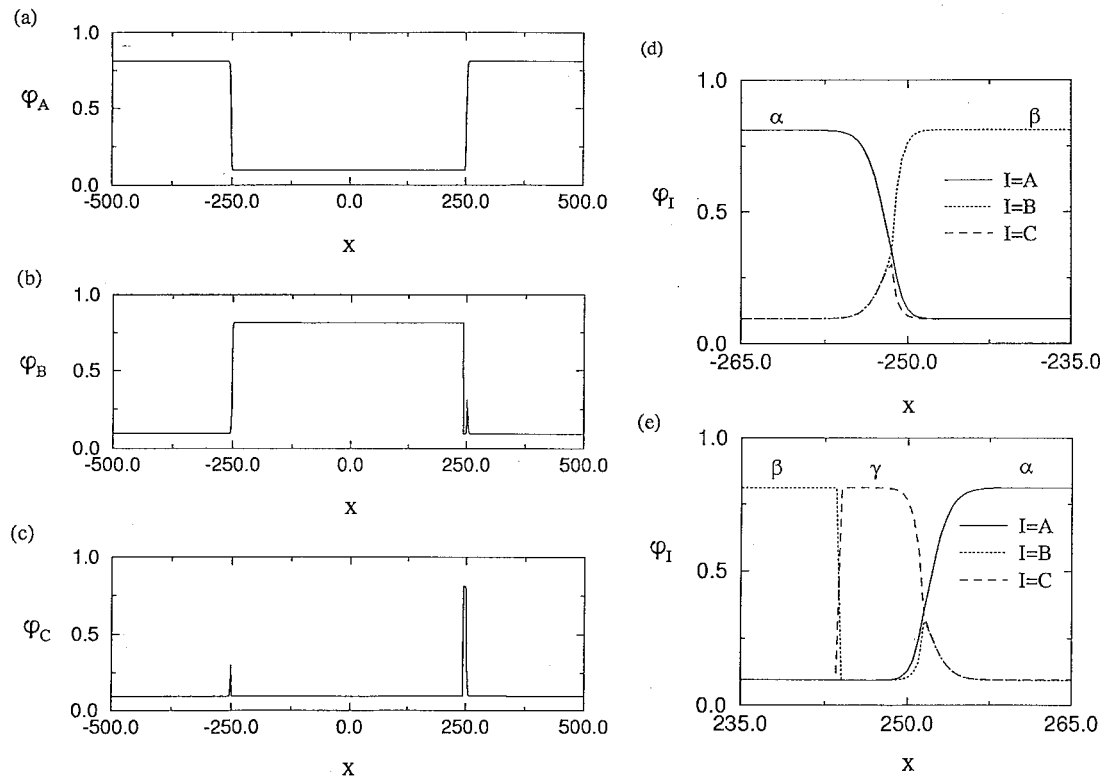

Fig. 3. Equilibrium composition profiles of system 6 in Fig. 1(d) for $e_1 = 0$ and $e_2 = 0$. The interfaces plotted in a larger scale are shown in parts (d) and (e). The values of x are in the unit of $(4\bar{\kappa}_{AA}/\omega)^{1/2}$.

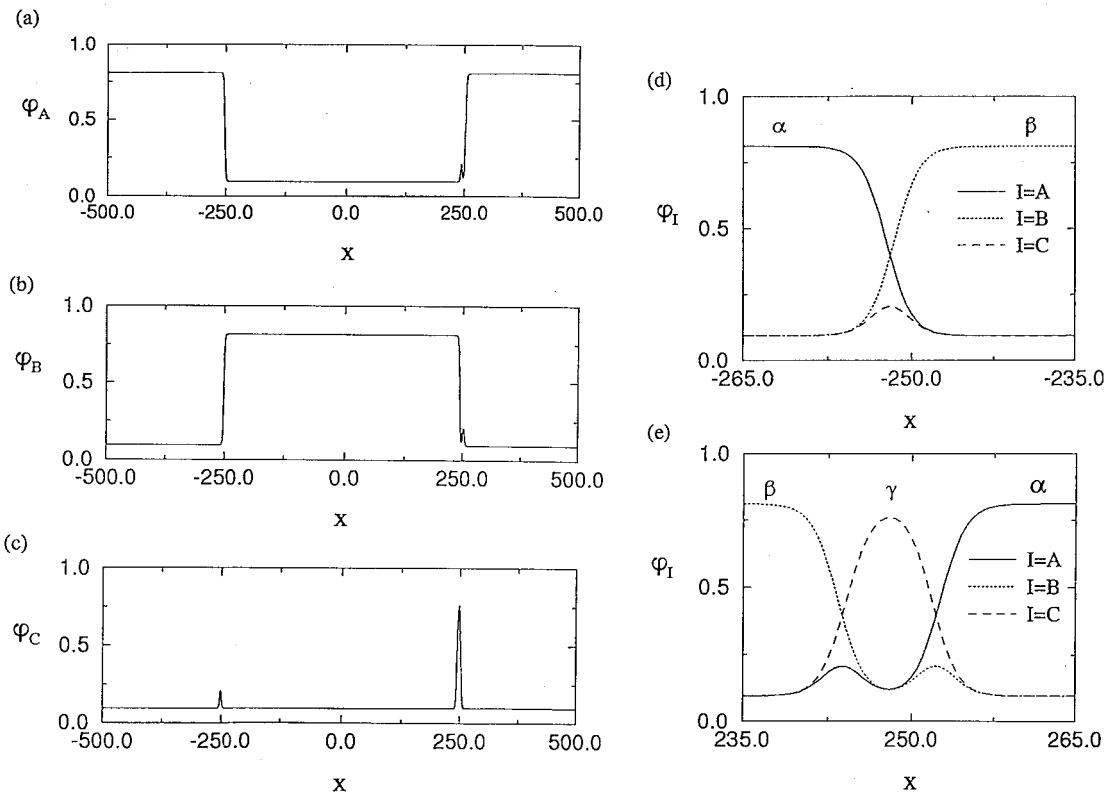

Fig. 4. Equilibrium composition profiles of system 6 in Fig. 1(d) for $e_1 = 1$ and $e_2 = 1$. The interfaces plotted in a larger scale are shown in parts (d) and (e). The values of x are in the unit of $(4\bar{\kappa}_{AA}/\omega)^{1/2}$.

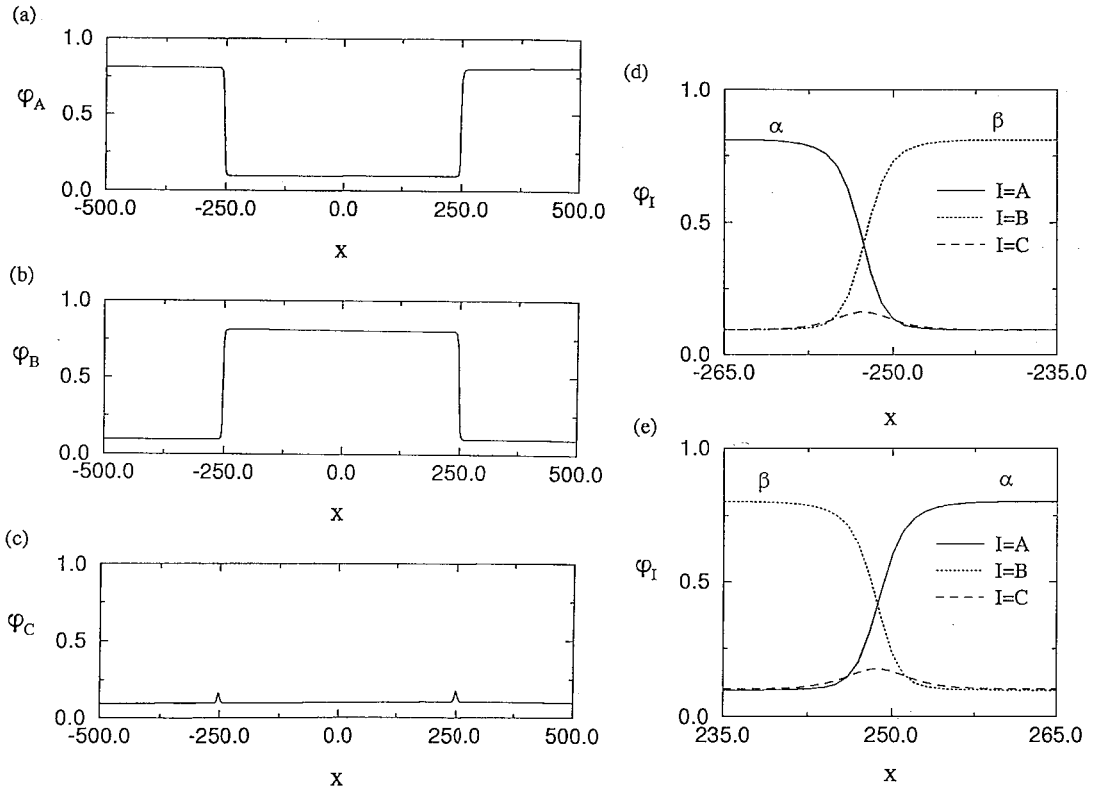

Fig. 5. Equilibrium composition profiles of system 6 in Fig. 1(d) for $e_1 = 1$ and $e_2 = 10$. The interfaces plotted in a larger scale are shown in parts (d) and (e). The values of x are in the unit of $(4\bar{\kappa}_{AA}/\omega)^{1/2}$.

α- and β-phases, and the adsorption of B between the α- and γ-phases. However, the component A does not segregate in the interfaces between the B-rich and the C-rich phases; even a small amount of A segregating in the interfaces increases the interfacial energy since $\bar{\kappa}_{BB} = \bar{\kappa}_{CC} = 0$. When all of $\bar{\kappa}_{II}$ are equal, i.e. $e_1 = e_2 = 1$, each component K segregates in the interfaces between the I-rich and J-rich phases (see Fig. 4). Note that there is still the formation of γ-phase, it does not reach the equilibrium compositions as given by the phase diagram. No adsorption of the A and B components is observed as $\bar{\kappa}_{CC}$ increases, as shown in Fig. 5, and the γ-phase seems to disappear since the maximum of the composition C is much smaller than the equilibrium composition given by the phase diagram.

In order to see if these results are due to the finite size effect, we determine the profiles of system 6 by doubling the size for $e_1 = e_2 = 1$, and $e_1 = 1$, $e_2 = 10$, respectively. That is, the initial amounts of the α-, β-, and γ-phases are doubled. In the case of $e_1 = e_2 = 1$, we observe that the compositions of the γ-phase reach the equilibrium compositions given by the phase diagram. While in the case of $e_1 = 1$ and $e_2 = 10$, the γ-phase comes closer to the equilibrium compositions but still does not attain the values given by the phase diagram. If, however, the system size is made still larger, the γ-phase will reach the equilibrium compositions given by the phase diagram. The dynamics (i.e. the solution of the NLCH equations in two dimensions) show that the third γ-phase always forms at the junctions of the interfaces between the α- and β-phases, where the nucleus rich in the minority C component reaches the equilibrium composition first. Therefore, it is much harder for the γ-phase to reach its equilibrium compositions when $\bar{\kappa}_{CC}$ is large.

It should be noted that in equilibrium due to the gradient energy coefficients, the γ-phase will not always form between the α- and β-phases. Consider two possible spatial distributions of the α-, β- and γ-phases: α–γ–β and γ–α–β with total interfacial energies σ_1 and σ_2, respectively. When there is no gradient coefficient for the C component (i.e. $\bar{\kappa}_{CC} = 0$), σ_1 is always less than σ_2 and therefore the formation of the γ-phase between the α- and β-phases is the most stable in this case. However, this is not the case if $\bar{\kappa}_{CC}$ is large. In this case σ_1 can be larger than σ_2, which implies that γ–α–β is the most stable configuration.

6. SUMMARY

The interface profiles of ternary alloys decomposed into two- and three-phase regions are obtained solving the non-linear Cahn–Hilliard equations (NLCH) in the steady-state limit. We

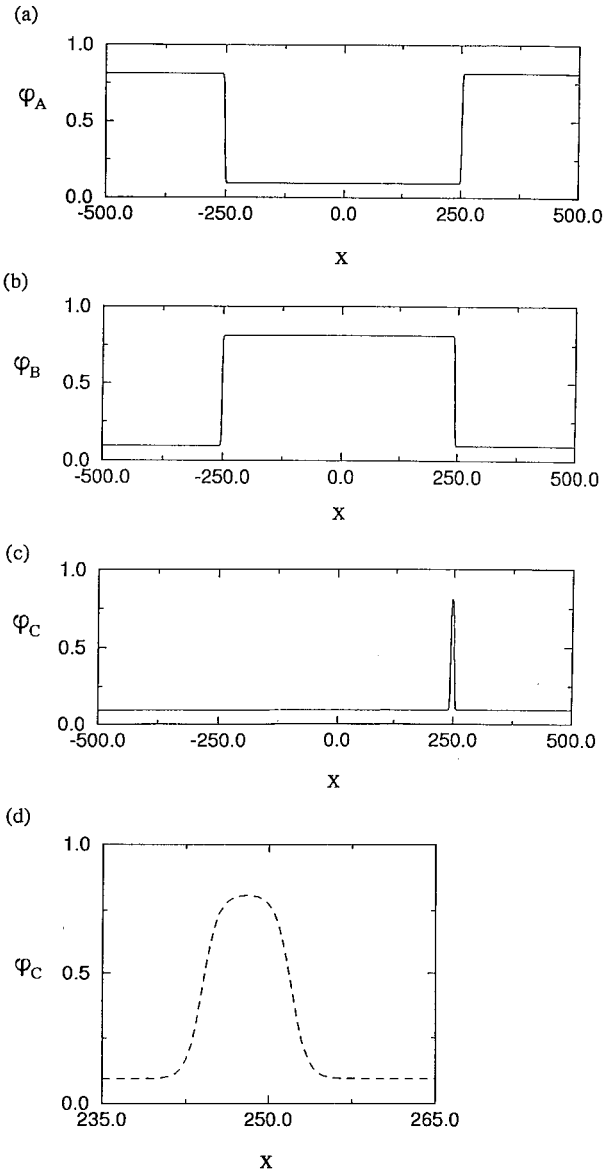

Fig. 6. Initial composition profiles of system 6 in Fig. 1(d). The initial γ-phase is enlarged in part (d). The values of x are in the unit of $(4\bar{\kappa}_{AA}/\omega)^{1/2}$.

also determine the interfacial energy minimizing composition profiles by solving the two Euler–Lagrange equations. We concluded that the steady-state solution of the NLCH equations are identical to the solutions obtained from the E–L equations for two-phase systems. In the three-phase systems, the NLCH approach is most efficient.

We study the effect of the gradient energy coefficients, $\bar{\kappa}_{II}$, on the two-phase and three-phase interface profiles. In ternary alloys with a minority component C, we find that $\bar{\kappa}_{CC}$ can have a strong influence on the degree of adsorption. In two-phase regions, the scaling of the maximum in $\Delta\varphi_C(x)$ is properly given by the Landau-type analysis near the critical points and when the gradient energy coefficients are large. Near the critical points Γ_C is independent of $\bar{\kappa}_{CC}$. This result is also true for conditions not near the critical point where the adsorption is small [9, 10]. As $\bar{\kappa}_{CC}$ decreases the maximum of $\Delta\varphi_C(x)$ increases leading to large degrees of the adsorption of C along the interfaces. In this case, as in deep quenches, only the non-linear E–L equations or the steady-state solution of the NLCH equations can give the interface profile. For a ternary system unstable to the formation of the two majority α- and β-phases and metastable to the formation of the third minority γ-phase, the γ-phase does not necessarily form between the α- and β-phases when $\bar{\kappa}_{CC}$ is large.

Acknowledgements—M.O. and C.H. acknowledge financial support from the National Science Foundation through

grant DMR-9509838, and the Ford Motor Co. P.V. acknowledges the financial support of the National Science Foundation through grant DMR-9707073.

REFERENCES

1. Hilliard, J. E., in *Phase Transformations*, ed. H. I. Aronson. American Society for Metals, Metals Park, OH, 1969.
2. Morral, J. E. and Cahn, J. W., *Acta metall. mater*., 1971, **19**, 1037.
3. de Fontaine, D., *J. Phys. Chem. Solids*, 1972, **33**, 297.
4. de Fontaine, D., *J. Phys. Chem. Solids*, 1973, **34**, 1285.
5. Chen, L. Q., *Scripta metall. mater*., 1993, **29**, 683.
6. Chen, L. Q., *Scripta metall. mater*., 1994, **42**, 3503.
7. Huang, C., Olvera de la Cruz, M. and Swift, B. W., *Macromolecules*, 1995, **28**, 7996.
8. Huang, C. and Olvera de la Cruz, M., *Phys. Rev. E*, 1996, **53**, 812.
9. Huang, C. and Olvera de la Cruz, M., *Europhys. Lett*., 1996, **34**, 171.
10. Huang, C. and Olvera de la Cruz, M., *Macromolecules*, 1996, **29**, 6068.
11. Eyre, D. J., in *Cascade of Spinodal Decomposition in the Ternary Cahn–Hilliard Equations in Mathematics of Microstructure Evolution*, ed. L.-Q. Chen, B. Fultz, J. Cahn, J. R. Manning, J. E. Morral and J. Simmons. TMS–SIAM, 1996.
12. Cahn, J. W. and Hilliard, J. E., *J. Chem. Phys*., 1958, **28**, 258.
13. Hildebrand, F. B., *Methods of Applied Mathematics*. Prentice-Hall, New York, 1992.
14. Ascher, U., Christiansen, J. and Russell, R. D., *Math. Comp*., 1979, **33**, 659.